Acta Mech
https://doi.org/10.1007/s00707-023-03499-1

ORIGINAL PAPER

Benjamin Hirzinger · **Udo Nackenhorst**

Efficient model-correction-based reliability analysis of uncertain dynamical systems

Received: 30 October 2022 / Revised: 12 December 2022 / Accepted: 13 January 2023

Abstract The scope of this paper is to apply a model-correction-based strategy for efficient reliability analysis of uncertain dynamical systems based on a low-fidelity (LF) model whose outcomes are corrected in a probabilistic sense to represent the more realistic outcomes of a high-fidelity (HF) model. In the model-correction approach utilized, the LF model is calibrated to the HF model close to the so-called most probable point in standard normal space, which allows a more realistic assessment of the considered complex dynamical system. Since only few expensive limit state function evaluations of the HF model are required, an efficient reliability analysis is enabled. In an application example, the LF model describes an existing single-span railway bridge modelled as simply supported Euler–Bernoulli beam subjected to moving single forces representing the axle loads of a moving train. The HF modelling approach accounts for the bridge–train interaction by modelling the passing train as mass-spring-damper system, however increasing the computational effort of the limit state function evaluations. Failure probabilities evaluated with the model-correction approach are contrasted and discussed with failure probabilities of the sophisticated bridge–train interaction model evaluated with the first-order reliability method (FORM). It is demonstrated that the efficiency of the method depends on the correlation between the LF and the HF model. A comparison of the results of FORM and the model-correction-based approach shows that the latter provides reliable failure probability prediction of the HF model while leading to a significant reduction in computational effort.

1 Introduction

Dynamical systems find a wide range of applications for problems involving response analysis, reliability assessment, and system control of engineering structures, biomechanical structures, and biological models, among others. Especially in civil engineering, structural responses of, for example, buildings, bridges, and offshore structures under time-dependent excitation are determined by dynamic simulations and subsequently the outcomes serve as basis for further performance analyses. In this context, reliability assessment of structures and the use of tailor made methods for reliability assessment is of great interest; however, as the behaviour of structures varies, identifying the most appropriate reliability assessment method is challenging. Recently, a lot

Benjamin Hirzinger and Udo Nackenhorst have contributed equally to this work.

B. Hirzinger (✉) · U. Nackenhorst
International Research Training Group (IRTG) 2657, Leibniz University Hannover, Appelstraße 11/11a, Hanover 30167, Lower Saxony, Germany
E-mail: benjamin.hirzinger@irtg2657.uni-hannover.de

B. Hirzinger · U. Nackenhorst
Institute of Mechanics and Computational Mechanics, Leibniz University Hannover, Appelstraße 9, Hanover 30167, Lower Saxony, Germany
E-mail: nackenhorst@ibnm.uni-hannover.de

Published online: 09 February 2023

of research is going on trying to provide optimal reliability assessment strategies for the system of interest. In [1], an active learning framework for solving complex reliability problems is discussed and 39 strategies for solving 20 reliability benchmark problems are investigated with the intention to provide recommendations for practitioners.

For linear and moderate nonlinear systems, the first-order reliability method (FORM) [2–4] is a well-established, fast, and accurate method with less limit state function evaluations required than, for example, crude Monte Carlo simulation (MCS). Based on a description of the reliability problem in standard Gaussian space, which requires the transformation of correlated non-Gaussian variables to uncorrelated Gaussian variables in FORM, the limit state function is linearized by a Taylor series approximation of first-order at the so-called most probable point (MPP) [4]. The evaluation of the most probable point, defined as point located to maximize the probability density function within the failure domain, requires solving a constrained optimization problem and subsequently enables the evaluation of the tail probability, respectively, the linearized systems failure probability [4–7]. The FORM method is widely used and has been applied, for example, for reliability assessment of a simply supported railway bridge [8]. Allahvirdizadeh et al. [8] focus on the reliability of an Euler–Bernoulli beam bridge model subjected to high-speed trains represented as moving static axle loads based on the bridge deck accelerations evaluated utilizing closed form solutions from literature. In [8], uncertain load models according to Annex E in Eurocode (EN) 1991-2 [9] are utilized for the response evaluation and omission sensitivity factors [10] are used as sensitivity measure of random variables depending on the limit state function.

In order to enhance the accuracy of FORM, principal curvatures at the MPP can be incorporated in the linear FORM approach for evaluating the failure probability leading to the second-order reliability method (SORM) [5,11–13]. For evaluating the failure probability, Breitung [11] derived an asymptotic equation that includes principal curvatures at the MPP and approaches the exact failure probability. In [14], a three-term approximation of the failure probability is presented in which the last two terms can be interpreted as extension of the asymptotic formula provided in [11]. Provided that the most probable point is accurately identified and unique, the FORM and SORM approximations have been shown by experience to be sufficiently accurate for engineering demands [15]. In [16], an extension of the first-order reliability method based on series expansion is provided for solving time-dependent reliability problems, also referred to as first passage problems. The widely used combination of the FORM method with Rice's formula (Rice/FORM method) for solving time-dependent reliability [17,18] is replaced by a combination of FORM and series expansion for enhancing accuracy and efficiency [16].

When dealing with highly nonlinear limit state functions which are typically only implicitly available e.g. by a finite element algorithm response surface methods (RSM)s can be applied with reasonable computational costs [4,19–21]. Commonly response surface models use first- or second-order polynomials as approximation function for the limit state function of the reliability problem in the region of the random variable space that has the most contribution to the probability of failure [20]. Consequently, the limit state function is expressed as an explicit function in dependence of the vector of basic random variables and conventional structural reliability methods such as FORM developed to deal with explicit limit state functions can then be used to compute structural failure probabilities at reduced computational cost [4].

Iourtchenko et al. [22] introduce a path integration method for strong nonlinear single-degree-of-freedom dynamical systems dealing with a first passage type reliability analysis. Therefore, the path integration method is adapted to first passage type reliability problems and tested on four different types of controlled systems, i.e. a system with dry friction and other three single-degree-of-freedom systems with parametric control of their parameters. The evaluation procedure is based on discrete versions of the Chapman–Kolmogorov equation enabling the determination of the response probability density function tails with high accuracy for small probabilities of failure ($< 10^{-6}$) and additionally providing first passage time statistics [22,23]. Recently, a Wiener path integral variational formulation with free boundaries for computationally efficient stochastic response evaluation of high-dimensional nonlinear dynamical systems is introduced in [24]. The proposed technique based on the Wiener path integral concept is capable of accurately determining the response probability density function of high-dimensional systems circumventing the curse of dimensionality at minimal computational cost.

Another approach to deal with complex systems represented by elaborate models that are highly computationally demanding is to incorporate knowledge of a simplified model following similar physical principles into the reliability evaluation process of the elaborate model. In [25], a survey on modern Monte Carlo methods for efficient uncertainty quantification and propagation is presented and in [26] so-called multifidelity methods for uncertainty propagation including multifidelity model management strategies are outlined. Peherstorfer et

al. [27] present a framework for multifidelity Monte Carlo estimation adopting an optimal model management strategy that decides which models to evaluate and when based on an optimization approach distributing the computational effort among the different models such that the mean squared error of the multifidelity estimator is minimized for a certain computational budget. This framework allows for a combination of an arbitrary number of surrogate models with different degree of sophistication and does not rely on a multilevel hierarchy with known error and cost rates. Typical surrogate models also referred to as low-fidelity (LF) models include projection-based reduced order models, data-fit models, machine learning-based models, e.g. neural networks, support vector machines, and simplified-physics models. A deep learning-based multifidelity surrogate model for robust aerodynamic design optimization is utilized in [28,29] using a multifidelity modelling framework based on recursive co-Kriging and Gaussian–Markov random fields. In [30], issues on the effective usage of multifidelity surrogates are discussed. Multifidelity modelling approaches for reliability estimation are discussed in [31] and an extension of the moving particles method [32,33] incorporating multifidelity models is provided in [34,35]. Proppe and Kaupp [36] present efficient multifidelity estimators for failure probabilities by combining additive and multiplicative information fusion with importance sampling and importance splitting. Recently, [37] propose an active learning multifidelity model framework for rare event simulation based on adaptive subset simulation. For robustly predicting small failure probabilities, the proposed framework uses a dynamic active learning function that decides when to call the high-fidelity (HF) model. Ditlevsen and Arnbjerg-Nielsen [38] propose a model-correction-factor method based on FORM that calibrates the reliability analysis procedure using outcomes of a simplified (LF) modelling approach with outcomes of a more sophisticated (HF) modelling approach in order to enhance the efficiency and accuracy of the reliability assessment. The LF model is calibrated to the HF model near the most probable point in standard normal space, which allows a more realistic assessment of the considered complex system [38]. In [39], the model-correction-factor method is applied to evaluate the reliability of a composite blade structure. As low-fidelity model of the blade profile, a cantilever Euler–Bernoulli beam is chosen, and as realistic model, a nonlinear shell-element finite element (FE) model is utilized. Dimitrov et al. [39] approximate the model-correction factor by a zero-order Taylor series expansion around the MPP and by a first-order Taylor series expansion around the MPP, respectively. It is shown that the first-order approximation is able to capture the influence of the parameters more accurately than the zero-order approximation in the application example. However, the first-order Taylor series approximation of the model-correction factor requires the evaluation of the gradient and therefore leads to significantly increased computational cost [39]. In case of the zero-order Taylor series expansion convergence was achieved after five iterations, consequently five limit state function evaluations of the elaborate nonlinear FE model are required. The first-order Taylor series expansion provided convergence after six iterations, leading to twelve limit state function in every iteration (one at the MPP and one additional call for each of the stochastic variables in order to determine the partial derivatives of the gradient) resulting in a twelve times higher computational effort for each iteration [39]. The model-correction-factor method is used by [40] for solving structural reliability problems where random fields are present in the definition of the limit state function. Based on the initial model-correction-factor framework, Alibrandi and Der Kiureghian [41] integrate a response surface technique and apply the enhanced methodology for evaluation of the design point and the FORM solution when dealing with nonlinear stochastic dynamic problems. Within the model-correction-based reliability analysis, framework efficient evaluation of failure probabilities based on a simplified model capturing basic structural behaviour is enabled while incorporating the modelling accuracy of a more sophisticated model. In comparison to response surface methods, in which even sophisticated techniques may require a substantial number of computationally challenging high-fidelity limit state function evaluations applying the model-correction-based approach the time-consuming HF model is evaluated only a few times until the LF model is calibrated.

In this study, the model-correction approach is utilized to conduct a reliability assessment of an simply supported railway bridge subjected to trains with high travelling speeds. As the dynamic behaviour of railway bridges is depending on multiple aspects such as boundary conditions [soil–structure interaction (SSI)], interaction between the bridge and the train (bridge–train interaction), among others, the underlying mechanical model capturing influential aspects is complex and should involve uncertainties treated as random variables [42–44]. The complex HF model utilized in this study explicitly accounts for SSI and bridge–train interaction, however the computational cost evaluating the limit state function is substantial. In an efficient simplified LF modelling approach the railway bridge is modelled as Euler–Bernoulli beam and the passing train is represented by its moving static axle loads [44], thus enabling efficient limit state function evaluations while incorporating the basic underlying physical behaviour of the complex system. It is shown that the model-correction-based

reliability assessment approach is able to efficiently predict failure probabilities of the complex system of interest.

2 Model-correction-based reliability analysis

In the context of a reliability analysis typically the probability of failure p_f of the considered system is of interest and uncertainties often associated with the structural loading, the material parameters of the structure, and environmental conditions, to name but a few are considered in the response evaluation procedure as random variables. Based on limit state function $g(\mathbf{X})$ with $\mathbf{X} = (X_1, X_2, \ldots, X_{N_\mathrm{r}})$ as random input vector including N_r random variables, that divides the basic variables space into a safe domain S ($g(\mathbf{X}) > 0$) and a failure domain F ($g(\mathbf{X}) \leq 0$) given a response limit state failure of a structure indicating a threshold exceedance can be expressed. Categorizing the random input variables into variables related with the structural demand $\mathbf{X}_S$ (load variables), variables related with the system capacity $\mathbf{X}_R$ (strength variables), and variables $\mathbf{X}_D$ related with the remaining parameters that do not necessarily have to be random the limit state function can be expressed with $\mathbf{X} = (\mathbf{X}_S, \mathbf{X}_R, \mathbf{X}_D)$ as $g(\mathbf{X}_S, \mathbf{X}_R, \mathbf{X}_D)$. Probability of failure p_f, defined as probability P that an undesired state is reached $p_\mathrm{f} = P(g(\mathbf{X}_S, \mathbf{X}_R, \mathbf{X}_D) \leq 0)$ can be computed as multifold integral of joint probability density function $f_\mathbf{X}$ over failure domain F: $p_\mathrm{f} = P(g(\mathbf{X}) \leq 0) = \int \cdots \int_F f_\mathbf{X}(\mathbf{x}) d\mathbf{x}$. Analytical solutions of the multifold integral exist for special cases only, numerical integration of the integral is computationally highly expansive, and it is difficult to appropriately locate integration points for numerical integration [4]. Consequently, Monte Carlo simulation is commonly applied to predict failure probabilities, however for complex limit state functions and small failure probabilities it becomes cumbersome whereas FORM and SORM are not strongly influenced by the order of the failures probability [7]. For linear and moderate nonlinear problems often FORM and SORM are straightforward failure probability evaluation techniques [4]. In case of correlated non-Gaussian input variables $\mathbf{X} = (X_1, X_2, \ldots, X_{N_\mathrm{r}})$, they need to be transformed as FORM and SORM involve uncorrelated Gaussian distributed input variables $\mathbf{U} = (U_1, U_2, \ldots, U_{N_\mathrm{r}})$ [7]. The constrained optimization problem of FORM and SORM provided in "Appendix A" can be solved using, for example, sequential quadratic programming (SQP) procedures [4] leading to the MPP $\mathbf{u}^*$ in standard normal space. Consequently, the failure probability is given as [4]

$$p_\mathrm{f} = \Phi(-\beta) \tag{1}$$

with standard normal cumulative distribution Φ and reliability index β representing the distance between $\mathbf{u}^*$ and the origin in standard normal space $\mathbf{O}$. In case of a linear system the FORM method provides the exact result of the failure probability p_f. In "Appendix A", a detailed outline of FORM is provided.

In order to achieve accurate and reliable results, it is desirable to represent the system of interest by a detailed high-fidelity (HF) analysis model. However, prediction of failure probabilities for computationally demanding analysis models becomes cumbersome when a substantial number of limit state function evaluations is required. In this section, a model-correction approach for efficient computation of failure probabilities for a complex high-fidelity (HF) analysis model is outlined, which is based on outcomes of a simplified (LF) modelling approach that captures the main physical properties of the system.

2.1 Model-correction-factor method

The limit state function of a HF model that defines the division of the entire space of basic variables in to a safe domain S_HF and a failure domain F_HF, respectively, can be represented with $\mathbf{x}_S$, $\mathbf{x}_R$, and $\mathbf{x}_D$ as samples of random variables $\mathbf{X}_S$, $\mathbf{X}_R$, and $\mathbf{X}_D$ by [38]

$$g_\mathrm{HF}(\mathbf{x}_S, \mathbf{x}_R, \mathbf{x}_D) = 0 \tag{2}$$

with $\mathbf{x}_S$ denoting the load or demand variables, $\mathbf{x}_R$ the strength or capacity variables, and $\mathbf{x}_D$ the remaining parameters. It should be noted that limit state function g_HF is not necessary provided in explicit form, it could be, for example, represented in implicit form by a finite element algorithm. The limit state function of a low-fidelity model [38]

$$g_\mathrm{LF}(\mathbf{x}_S, \mathbf{x}_R, \mathbf{x}_D) = 0 \tag{3}$$

divides the space in an safe domain S_{LF} ($g_{\mathrm{LF}} > 0$) and a failure domain F_{LF} ($g_{\mathrm{LF}} \leq 0$) and is considered to be a less-elaborate function than g_{HF}. For evaluation of the failure probability $P(F_{\mathrm{HF}})$, it is desirable to incorporate basic physical information provided by the LF model, such that $P(F_{\mathrm{HF}})$ can be determined with less computational cost. Assuming star-shaped safe sets (S_{LF} and S_{HF}) in terms of $\mathbf{x}_S$ with respect to the origin of $\mathbf{x}_S$ for the HF model and the LF model, respectively, for any $\mathbf{x}_S, \mathbf{x}_R, \mathbf{x}_D$ the following equations [38]

$$g_{\mathrm{HF}}(\kappa_{\mathrm{HF}}\mathbf{x}_S, \mathbf{x}_R, \mathbf{x}_D) = 0 \tag{4}$$

$$g_{\mathrm{LF}}(\kappa_{\mathrm{LF}}\mathbf{x}_S, \mathbf{x}_R, \mathbf{x}_D) = 0 \tag{5}$$

have a unique solution with respect to capacity factor κ_{HF} and κ_{LF}, respectively. Due to the homogeneity of physical dimension of (2) and (3), respectively, limit state function g_{HF} [Eq. (2)] is equal to [38]

$$g_{\mathrm{LF}}(\mathbf{x}_S, \nu(\mathbf{x})\mathbf{x}_R, \mathbf{x}_D) = 0 \tag{6}$$

With $\kappa_{\mathrm{HF}}(\mathbf{x})$ and $\kappa_{\mathrm{LF}}(\mathbf{x})$ providing unique solutions of (4) and (5) effectivity factor $\nu(\mathbf{x}) = \frac{\kappa_{\mathrm{HF}}(\mathbf{x})}{\kappa_{\mathrm{LF}}(\mathbf{x})}$ with $\mathbf{x} = (\mathbf{x}_S, \mathbf{x}_R, \mathbf{x}_D)$ is defined. As the two models describe the same physical phenomenon and consequently qualitatively behave in a similar manner, it is reasonable to assume that $\nu(\mathbf{x})$ can be locally approximated by a constant ν^* [38,41]. Subsequently, resulting in the zero-order corrected idealized model $g_{\mathrm{LF}}(\mathbf{x}_S, \nu^*\mathbf{x}_R, \mathbf{x})_D = 0$. Commonly $\nu(\mathbf{x})$ is approximated at the MPP of the HF model $\nu(\mathbf{u}^*_{\mathrm{HF}}) = \nu^*$. The task is to find a value for ν^* such that the MPP of the corrected LF model $\mathbf{u}^*_{\mathrm{LF}}$ is as close as possible to the target MPP of the HF model $\mathbf{u}^*_{\mathrm{HF}}$. A detailed outline of the algorithm finding the optimal ν^* based on the first-order reliability method (FORM) is provided in [38].

2.2 Adaption to time-dependent systems

Assuming an uncertain structural system under time-dependent excitation $F(t)$ and introducing random vector $\mathbf{u}$, with $\mathbf{u} = (u_1, u_2, \ldots, u_{N_{\mathrm{r}}})$ comprised of samples of N_{r} independent standard normal random variables the time-dependent response of stochastic nature can be denoted as $Z(t, \mathbf{u})$. Given a limit state γ and time t the failure probability of the dynamical system is given as $p_{\mathrm{f}} = P(\gamma \leq Z(t, \mathbf{u}))$. A FORM solution is constructed by defining the limit state function $g(\mathbf{u}, \gamma, t) = \gamma - Z(t, \mathbf{u})$ and finding MPP $\mathbf{u}^*$ by solving the constrained optimization problem, providing a first-order approximation of the tail probability $p_{\mathrm{f}} = P[\gamma \leq Z(t, \mathbf{u})] \approx \Phi[-\beta(\gamma, t)]$. A detailed outline is provided in "Appendix A".

Interpreting the demand variables $\mathbf{x}_s$ as time history response $Z(t, \mathbf{u})$, the time-dependent limit state function g_{HF} of the HF model [Eq. (2)] reads [41]

$$g_{\mathrm{HF}}(Z_{\mathrm{HF}}(t, \mathbf{u}), \gamma) = \gamma - Z_{\mathrm{HF}}(t, \mathbf{u}) \tag{7}$$

and time-dependent limit state function g_{LF} of the simplified LF model is given as [41],

$$g_{\mathrm{LF}}(Z_{\mathrm{LF}}(t, \mathbf{u}), \gamma) = \gamma - Z_{\mathrm{LF}}(t, \mathbf{u}) \ , \tag{8}$$

respectively, where the response threshold γ can be considered as a capacity variable. Introducing capacity factors κ_{HF} and κ_{LF} [41], yields

$$g_{\mathrm{HF}}(Z_{\mathrm{HF}}(t, \mathbf{u}), \kappa_{\mathrm{HF}}\gamma) = \kappa_{\mathrm{HF}}\gamma - Z_{\mathrm{HF}}(t, \mathbf{u}) \tag{9}$$

and

$$g_{\mathrm{LF}}(Z_{\mathrm{LF}}(t, \mathbf{u}), \kappa_{\mathrm{LF}}\gamma) = \kappa_{\mathrm{LF}}\gamma - Z_{\mathrm{LF}}(t, \mathbf{u}) \tag{10}$$

In equivalence to Sect. 2.1, a unique solution of the limit state function g_{HF} [Eq. (7)] and g_{LF} [Eq. (8)] with respect to capacity factor $\kappa_{\mathrm{HF}}(\mathbf{u}) = \frac{Z_{\mathrm{HF}}(t,\mathbf{u})}{\gamma}$ and $\kappa_{\mathrm{LF}}(\mathbf{u}) = \frac{Z_{\mathrm{LF}}(t,\mathbf{u})}{\gamma}$ is assumed, leading to effectivity factor $\nu(\mathbf{u})$ of the uncertain dynamical models given as [41],

$$\nu(\mathbf{u}) = \frac{\kappa_{\mathrm{HF}}(\mathbf{u})}{\kappa_{\mathrm{LF}}(\mathbf{u})} = \frac{Z_{\mathrm{HF}}(t, \mathbf{u})}{Z_{\mathrm{LF}}(t, \mathbf{u})} \tag{11}$$

Consequently, the corrected LF model is defined as the original LF model with the demand random variable corrected by effectivity factor $\nu(\mathbf{u})$ [41], yielding

$$g_{\mathrm{LF}}(\nu(\mathbf{u})Z_{\mathrm{LF}}(t,\mathbf{u}),\gamma) = \gamma - \nu(\mathbf{u})Z_{\mathrm{LF}}(t,\mathbf{u}) \tag{12}$$

By inserting Eq. (11) in Eq. (12), it can be shown that the corrected LF model is equivalent to the HF model [41]

$$g_{\mathrm{LF}}(\nu(\mathbf{u})Z_{\mathrm{LF}}(t,\mathbf{u}),\gamma) = \gamma - \frac{Z_{\mathrm{HF}}(t,\mathbf{u})}{Z_{\mathrm{LF}}(t,\mathbf{u})}Z_{\mathrm{LF}}(t,\mathbf{u}) \tag{13}$$

$$= \gamma - Z_{\mathrm{HF}}(t,\mathbf{u}) \mathrel{\widehat{=}} g_{\mathrm{HF}}(Z_{\mathrm{HF}}(t,\mathbf{u}),\gamma) \tag{14}$$

The zero-order corrected LF model is obtained by approximation of $\nu(\mathbf{u})$ with constant ν^* [41], yielding

$$g_{\mathrm{LF}}(\nu^* Z_{\mathrm{LF}}(t,\mathbf{u}),\gamma) = \gamma - \nu^* Z_{\mathrm{LF}}(t,\mathbf{u}) \tag{15}$$

Consequently, a FORM-based algorithm can be utilized in order to find an optimal value for ν^* such that the MPP $\mathbf{u}^*_{\mathrm{LF}}$ of the LF model is as close as possible to the MPP of the HF model $\mathbf{u}^*_{\mathrm{HF}}$ [41].

2.3 Algorithm of model-correction-based reliability analysis

In a first step, an initial value for $\mathbf{u}^{(0)}_{\mathrm{LF}}$ is chosen and $\kappa^{(1)}_{\mathrm{LF}}$ is set to 1. Next utilizing Eq. (9) an initial estimate of $\kappa^{(1)}_{\mathrm{HF}} = Z_{\mathrm{HF}}(t,\mathbf{u}^{(0)}_{\mathrm{LF}})/x$ is determined. Based on a first estimate of the model-correction factor $\nu^{(1)} = \kappa^{(1)}_{\mathrm{HF}}/\kappa^{(1)}_{\mathrm{LF}}$ the corresponding corrected low-fidelity model $g^{(1)}_{\mathrm{LF}} = x - \nu^{(1)}Z_{\mathrm{LF}}(t,\mathbf{u})$ is solved by FORM providing $\mathbf{u}^{(1)}_{\mathrm{LF}}$ and $\beta^{(1)}_{\mathrm{LF}}$ [38]. Using $\mathbf{u}^{(1)}_{\mathrm{LF}}$ and repeating the outlined analysis steps, $\kappa^{(2)}_{\mathrm{HF}} = Z_{\mathrm{HF}}(t,\mathbf{u}^{(1)}_{\mathrm{LF}})/x$, $\nu^{(2)} = \kappa^{(2)}_{\mathrm{HF}}/\kappa^{(2)}_{\mathrm{LF}}$, and applying FORM on $g^{(2)}_{\mathrm{LF}} = x - \nu^{(2)}Z_{\mathrm{LF}}(t,\mathbf{u})$ provides $\mathbf{u}^{(2)}_{\mathrm{LF}}$ and $\beta^{(2)}_{\mathrm{LF}}$. Consequently, proceeding with the previous procedure results in a set of $(\kappa^{(1)}_{\mathrm{HF}},\hat{\beta}^{(1)}_{\mathrm{HF}}),(\kappa^{(2)}_{\mathrm{HF}},\hat{\beta}^{(2)}_{\mathrm{HF}}),\ldots,(\kappa^{(k)}_{\mathrm{HF}},\hat{\beta}^{(k)}_{\mathrm{HF}})$. In case of convergence, $\kappa^{(k)}_{\mathrm{HF}} \to 1$, $\hat{\beta}^{(k)}_{\mathrm{HF}} \to \hat{\beta}_{\mathrm{HF}}$, $\hat{\mathbf{u}}^{(k)}_{\mathrm{HF}} \to \hat{\mathbf{u}}^*_{\mathrm{HF}}$, with $k = 1,2,\ldots$, the most probable point of the corrected low-fidelity model $\hat{\mathbf{u}}^*_{\mathrm{HF}}$, and the corresponding reliability index $\hat{\beta}_{\mathrm{HF}}$. Due to $\kappa_{\mathrm{HF}} = 1$, $\hat{\mathbf{u}}^*_{\mathrm{HF}}$ is located on the limit state surface of the high-fidelity model. As a consequence of the corrected MPP of the LF model $\mathbf{u}^*$ being on the limit state surface of both the low-fidelity model and the high-fidelity model, the corresponding reliability index β_{LF} is an upper bound to the reliability index of the high-fidelity system [41]. In Fig. 1, a flowchart of the model-correction-based reliability approach is depicted.

Assuming that the response of the low-fidelity model is close to the response of the realistic high-fidelity model, it can be concluded that $\mathbf{u}^*_{\mathrm{LF}}$ is close to the target $\mathbf{u}^* = \mathbf{u}^*_{\mathrm{HF}}$. No convergence of the algorithm indicates that the low-fidelity model is not representing the main behaviour of the high-fidelity model and consequently an adapted simplified model should be chosen [41].

3 Application example

In this section, the model-correction-based analysis approach is performed in order to evaluate failure probabilities of an existing railway bridge subjected to a moving train. Two different modelling approaches with different degree of sophistication are applied. In the simplified LF approach, the railway bridge is modelled as Euler–Bernoulli beam bridge passed by moving single forces representing the axle loads of a moving train. The sophisticated HF modelling approach explicitly considers bridge–train interaction effects by modelling the passing train as mass-spring-damper (MSD) system.

3.1 Multifidelity modelling approach

The Euler–Bernoulli beam bridge model representing a single-span railway bridge can be mathematically expressed by the partial differential equation of motion [45]

$$\rho A\ddot{w}(x,t) + \mathrm{EI}w_{,xxxx}(x,t) = f(x,t) \tag{16}$$

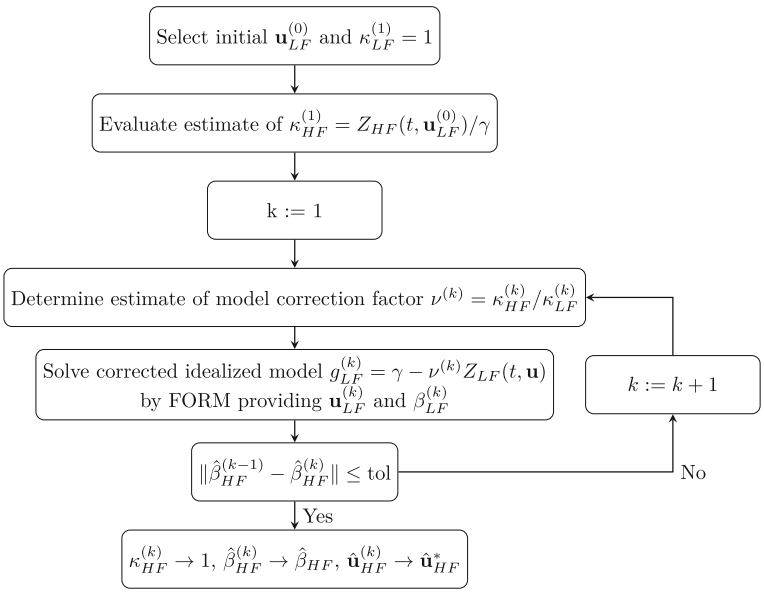

Fig. 1 Flow of the model-correction-based reliability approach

with $w(x,t)$ denoting the vertical beam bridge displacement at point x and time t. Extended boundary conditions of the Euler–Bernoulli beam (cf. Fig. 2), which take into account the influence of soil–structure interaction (SSI), result in the beam being non-classically damped and therefore a complex modal analysis is used to evaluate structural responses. Rearranging Eq. (16) and adding the identity $\rho A v(x,t) = \rho A \dot{w}(x,t)$ yields the initial partial differential equation Eq. (16) transformed into state-space [46],

$$\mathbf{E}\hat{x}(x,t) + \mathbf{F}\dot{\hat{x}}(x,t) = \mathbf{p}(x,t) \tag{17}$$

with

$$\hat{\mathbf{x}} = \begin{bmatrix} w(x,t) \\ v(x,t) \end{bmatrix}, \quad \mathbf{E} = \begin{bmatrix} \mathrm{EI}\frac{\partial^4}{\partial x^4} & 0 \\ 0 & -\rho A \end{bmatrix}, \quad \mathbf{F} = \begin{bmatrix} 0 & \rho A \\ \rho A & 0 \end{bmatrix}, \quad \mathbf{p} = \begin{bmatrix} f(x,t) \\ 0 \end{bmatrix} \tag{18}$$

Modal expansion of state-space vector $\hat{\mathbf{x}}(x,t)$ [46]

$$\hat{\mathbf{x}} = \sum_{r=1}^{\infty} x_r^*(t) \begin{bmatrix} \Phi_r(x) \\ \Phi_r(x) s_r \end{bmatrix} + \sum_{r=1}^{\infty} \bar{x}_r^*(t) \begin{bmatrix} \bar{\Phi}_r(x) \\ \bar{\Phi}_r(x) \bar{s}_r \end{bmatrix} = 2\mathcal{R}\left(\sum_{r=1}^{\infty} x_r^*(t) \begin{bmatrix} \Phi_r(x) \\ \Phi_r(x) s_r \end{bmatrix} \right) \tag{19}$$

leads in combination with the two orthogonality relations in state-space (cf. [46]) to the following ordinary decoupled modal differential equations [46],

$$a_r \dot{x}_r^*(t) + b_r x_r^*(t) = f_r(t)\,, \;\; \bar{a}_r \dot{\bar{x}}_r^*(t) + \bar{b}_r \bar{x}_r^*(t) = \bar{f}_r(t) \tag{20}$$

with $\bar{x}_r^*(t)$, $\bar{a}_r$, $\bar{b}_r$, $\bar{f}_r$ as complex conjugates of x_r^*, a_r, b_r, and f_r.

In a simplified modelling approach, the moving train is considered as moving single forces representing the static axle loads of the train (cf. Fig. 2) with the load function of the time dependent forces [46]

$$f(x,t) = \sum_{i=1}^{N_w} F_b^{(i)}(t) \delta(x - \xi_i(t)) \Pi\left(t, t_i^{(B)}, t_i^{(C)}\right) \tag{21}$$

controlling the amplitude and location of the moving forces on the beam bridge, as well as their appearance and disappearance [46]. In Eq. (21), Dirac delta function $\delta(x - \xi_i(t))$ denotes the i-th force with amplitude $F_b^{(i)}(t)$ at position $\xi_i(t) (= vt - l_i)$. This force enters the beam at time $t_i^{(B)} = l_i/v$ and leaves the beam at time $t_i^{(C)} = (l_i + L)/v$, controlled by the Heaviside functions $H(t - t_i^{(B)})$ and $H(t - t_i^{(C)})$, respectively,

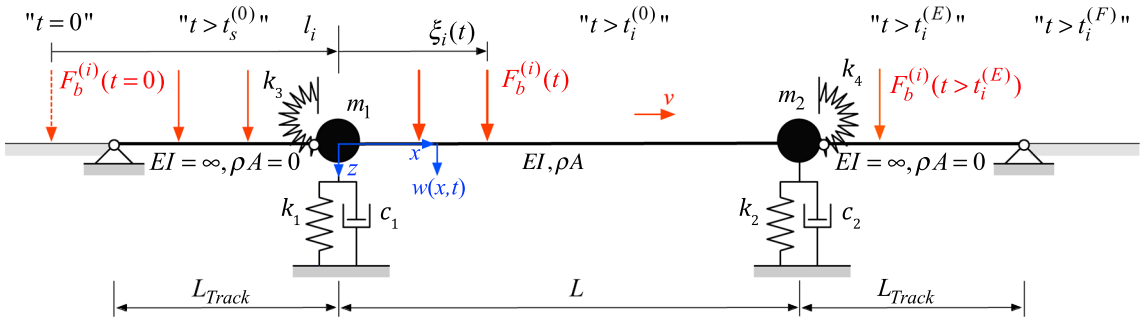

Fig. 2 Euler–Bernoulli beam bridge model subjected to the moving single axle load $F_b^{(i)}$ with constant speed v, modified from [46]

i.e. $\Pi(t, t_i^{(B)}, t_i^{(C)}) = H(t - t_i^{(B)}) - H(t - t_i^{(C)})$. The r-th modal load f_r reads in general form $f_r(t) = \int_L \Phi_r(x) f(x,t) \mathrm{d}x$ [46]. Evaluation of this relation for the assembly of the N_w moving single forces passing the beam bridge described by Eq. (21) yields the following expression for the r-th modal load on the beam bridge [46],

$$\begin{aligned} f_b^{(r)}(t) &= \int_L \sum_{i=1}^{N_w} F_b^{(i)}(t)\delta(x - \xi_i)\Pi\left(t, t_i^{(B)}, t_i^{(C)}\right)\Phi_r(x)\mathrm{d}x \\ &= \sum_{i=1}^{N_w} F_b^{(i)}(t)\Pi\left(t, t_i^{(B)}, t_i^{(C)}\right)\Phi_r(\xi_i) \end{aligned} \tag{22}$$

The effect of the train before arriving on the beam bridge and after leaving the beam bridge is considered in the modelling approach and is outlined in detail in [46]. Consequently, the r-th modal load reads $f_r = f_0^{(r)} + f_b^{(r)} + f_L^{(r)}$ [46].

Considering the first N_Φ modes, the modal state-space equations of motion Eqs (20) of the Euler–Bernoulli beam read [46]

$$\mathbf{A}_b\dot{\mathbf{x}}^* + \mathbf{B}_b\mathbf{x}^* = \mathbf{f}_b^* \tag{23}$$

with $\mathbf{x}^* = [x_1^*, \ldots, x_r^*, \ldots, x_{N_\Phi}^*, \bar{x}_1^*, \ldots, \bar{x}_r^*, \ldots, \bar{x}_{N_\Phi}^*]^{\mathrm{T}}$, $\mathbf{A}_b = \mathrm{diag}[a_1, \ldots, a_r, \ldots, a_{N_\Phi}, \bar{a}_1, \ldots, \bar{a}_r, \ldots, \bar{a}_{N_\Phi}]$, $\mathbf{B}_b = \mathrm{diag}[b_1, \ldots, b_r, \ldots, b_{N_\Phi}, \bar{b}_1, \ldots, \bar{b}_r, \ldots, \bar{b}_{N_\Phi}]$, and $\mathbf{f}_b^* = [f_1, \ldots, f_r, \ldots, f_{N_\Phi}, \bar{f}_1, \ldots, \bar{f}_r, \ldots, \bar{f}_{N_\Phi}]^{\mathrm{T}}$. This set of decoupled ordinary first-order differential equations is solved by time integration. Since Eq. (20) appear in complex conjugate pairs, $x^* + \bar{x}^* = 2\mathcal{R}(x^*)$ applies. The system responses beam displacement $w(x,t)$, velocity $\dot{w}(x,t)$, and acceleration $\ddot{w}(x,t)$ are consequently obtained by approximating the modal series by N_Φ modes [46],

$$\begin{aligned} w(x,t) &\approx \sum_{r=1}^{N_\Phi}\Phi_r(x)x_r^*(t) + \sum_{r=1}^{N_\Phi}\bar{\Phi}_r(x)\bar{x}_r^*(t) = 2\mathcal{R}\left\{\sum_{r=1}^{N_\Phi}\Phi_r(x)x_r^*(t)\right\}, \\ \dot{w}(x,t) &\approx \sum_{r=1}^{N_\Phi}\Phi_r(x)\dot{x}_r^*(t) + \sum_{r=1}^{N_\Phi}\bar{\Phi}_r(x)\dot{\bar{x}}_r^*(t) = 2\mathcal{R}\left\{\sum_{r=1}^{N_\Phi}\Phi_r(x)\dot{x}_r^*(t)\right\}, \\ \ddot{w}(x,t) &\approx \sum_{r=1}^{N_\Phi}\Phi_r(x)s_r\dot{x}_r^*(t) + \sum_{r=1}^{N_\Phi}\bar{\Phi}_r(x)\bar{s}_r\dot{\bar{x}}_r^*(t) = 2\mathcal{R}\left\{\sum_{r=1}^{N_\Phi}\Phi_r(x)s_r\dot{x}_r^*(t)\right\} \end{aligned} \tag{24}$$

The elaborate HF model considers the moving train as MSD system, consequently accounting for effects of bridge–train interaction (cf. Fig. 3). Based on the substructure approach, the equations of motion are specified for both the bridge and the train subsystem model separately, and then coupled by imposing coupling conditions at the interface of the subsystems. The N_c vehicles of the train subsystem are modelled as planar MSD systems

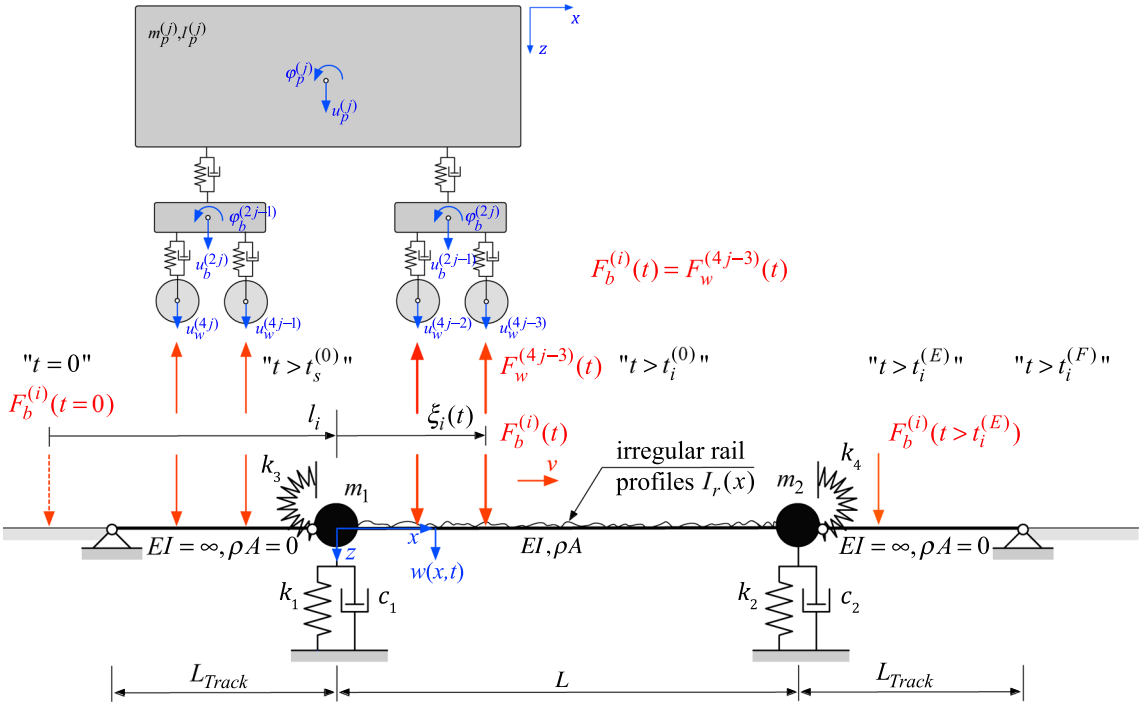

Fig. 3 Viscoelastically supported Euler–Bernoulli beam model and planar MSD model, modified form [46]

consisting of rigid bodies with mass, which represent passenger stage, two bogies and and four wheel pairs, connected by spring-dashpot elements. The equations of motion of a planar MSD subsystem read as [47],

$$\mathbf{M}_c\ddot{\mathbf{u}}_c + \mathbf{C}_c\dot{\mathbf{u}}_c + \mathbf{K}_c\mathbf{u}_c = \mathbf{F}_c \tag{25}$$

where $\mathbf{M}_c$ is the mass matrix, $\mathbf{C}_c$ is the damping matrix, and $\mathbf{K}_c$ is the stiffness matrix of the MSD subsystem. In the corresponding state-space representation [48],

$$\mathbf{A}_c\dot{\mathbf{d}}_c(t) + \mathbf{B}_c\mathbf{d}_c(t) = \mathbf{f}_c(t) \tag{26}$$

with the matrices $\mathbf{A}_c$, $\mathbf{B}_c$, and vector $\mathbf{f}_c$

$$\mathbf{A}_c = \begin{bmatrix} \mathbf{C}_c & \mathbf{M}_c \\ \mathbf{I}_c & \mathbf{0} \end{bmatrix}, \quad \mathbf{B}_c = \begin{bmatrix} \mathbf{K}_c & \mathbf{0} \\ \mathbf{0} & -\mathbf{I}_c \end{bmatrix}, \quad \mathbf{f}_c = \begin{bmatrix} \mathbf{F}_c \\ \mathbf{0} \end{bmatrix} \tag{27}$$

and the identity matrix $\mathbf{I}_c$, vector $\mathbf{d}_c = \{\mathbf{u}_c^{(1)}, \ldots, \mathbf{u}_c^{(j)}, \ldots, \mathbf{u}_c^{(N_c)}, \dot{\mathbf{u}}_c^{(1)}, \ldots, \dot{\mathbf{u}}_c^{(j)}, \ldots, \dot{\mathbf{u}}_c^{(N_c)}\}^{\mathrm{T}}$ contains all DOFs of the MSD system and their first derivative in time [46].

In the next step, the equations of motion in state-space of both subsystems are coupled using the so-called generalized corresponding assumption and applying a dynamic substructure technique (DST) in which the involved DOFs are condensed into the modal coordinates of the beam bridge model [46]. In vertical direction, it is assumed that the displacement of the beam and the MSD system at the point of contact are equal, and consequently, lift-off of the wheels is not admitted. The generalized corresponding assumption yields for the vertical displacement $u_w^{(i)}$ of the i-th wheel, which is at time t at position $\xi_i(t)$, together with Eq. (24) the following expression [46],

$$u_w^{(i)}(\xi_i) = w(\xi_i, t) + I_r(\xi_i) \approx \sum_{r=1}^{N_\Phi} \Phi_r(\xi_i) y_r(t) + \sum_{r=1}^{N_\Phi} \bar{\Phi}_r(\xi_i)\bar{y}_r(t) + I_r(\xi_i) \tag{28}$$

The variable $I_r(\xi_i = vt - l_i)$ represents a random irregularity profile function, which is applied to the beam surface to consider the effect of track irregularities, cf. Fig. 3. The transformation according to [46]

$$\begin{aligned} \mathbf{x}(t) &= \mathbf{\Gamma}_1(t)\mathbf{x}^*(t) + \mathbf{\Gamma}_2(t)\dot{\mathbf{x}}^*(t) + \mathbf{\Upsilon}(t), \quad \mathbf{x}^*(t) = \left[\mathbf{y}, \tilde{\mathbf{d}}_c\right]^{\mathrm{T}} \\ \dot{\mathbf{x}}(t) &= \dot{\mathbf{\Gamma}}_1(t)\mathbf{x}^*(t) + \mathbf{\Gamma}_1(t)\dot{\mathbf{x}}^*(t) + \dot{\mathbf{\Gamma}}_2(t)\dot{\mathbf{x}}^*(t) + \mathbf{\Gamma}_2(t)\ddot{\mathbf{x}}^*(t) + \dot{\mathbf{\Upsilon}}(t) \end{aligned} \tag{29}$$

with $\mathbf{\Gamma}_1(t)$ and $\mathbf{\Gamma}_2(t)$ as time-dependent transformation matrices, imposes the corresponding assumption Eq. (28) on the two subsystems, which are consolidated [46]. Consequently, the equations of motion in state-space of the coupled beam-MSD system reads [46],

$$\mathbf{A}^*(t)\dot{\mathbf{x}}^*(t) + \mathbf{B}^*(t)\mathbf{x}^*(t) = \mathbf{f}^*(t) \tag{30}$$

with the time-dependent system matrices

$$\begin{aligned} \mathbf{A}^*(t) &= \mathbf{\Gamma}_1^{\mathrm{T}}(t)\left[\mathbf{A}\mathbf{\Gamma}_1(t) + \mathbf{A}\dot{\mathbf{\Gamma}}_2(t) + \mathbf{A}\mathbf{\Gamma}_2(t)\mathbf{S} + \mathbf{B}\mathbf{\Gamma}_2(t)\right] , \\ \mathbf{B}^*(t) &= \mathbf{\Gamma}_1^{\mathrm{T}}(t)\left[\mathbf{A}\dot{\mathbf{\Gamma}}_1(t) + \mathbf{B}\mathbf{\Gamma}_1(t)\right] \end{aligned} \tag{31}$$

and

$$\mathbf{f}^*(t) = \mathbf{\Gamma}_1^{\mathrm{T}}(t)\left[\mathbf{f}(t) - \mathbf{A}\dot{\mathbf{\Upsilon}}(t) - \mathbf{B}\mathbf{\Upsilon}(t)\right] \tag{32}$$

The state-space solution vector $\mathbf{x}^*$ is computed by time integration using seven modes (i.e. $N_\Phi = 7$). For a detailed outline of the elaborate modelling strategy, it is referred to [43,46,47].

3.2 Considered bridge and subsoil, uncertainties, and limit state

The analysed single-span railway bridge is a ballasted steel bridge of span $L = 16.8$ m with bending stiffness $\mathrm{EI} = 3.262 \times 10^{10}$ Nm^2 and mass per unit length $\rho A = 1.220 \times 10^4$ kg/m. Natural frequencies of the beam bridge are $f_1 = 9.10$ Hz, $f_2 = 36.4$ Hz, $f_3 = 81.9$ Hz, $f_4 = 145$ Hz, $f_5 = 227$ Hz, $f_6 = 327$ Hz, and $f_7 = 445$ Hz. The considered train is the Austrian high-speed train Railjet with a configuration of one power car and seven passenger cars whose parameters, i.e. mass matrix $\mathbf{M}_c$, damping matrix $\mathbf{C}_c$, stiffness matrix $\mathbf{K}_c$ are provided in [42]. It should be noted that at a critical train speed, defined as $v_l^{(r)} = df_r/l\ ,\ \ l = 1, 2, 3, \ldots$, the r-th natural bridge frequency $f_r = \omega_r/(2\pi)$ is excited to a state of resonance due to the repetitive axle loads with constant distance d [49]. This distance corresponds to wagon length $d = 16.5$ m for the Railjet train. Uncertainties that are included in the system response evaluation are the structural parameters, structural damping ζ, moment of inertia I of the bridge beam, and parameters describing the subsoil quality comprised of subsoil Young's modulus E_s, subsoil Poisson's ration ν_s, subsoil density ρ_s, and the bedding stiffness $\bar{k}$ related with the subsoil [46]. Sources of energy dissipation in the bridge, for example, inherent structural damping, material damping, and viscous elements of the track are captured globally by a modal damping coefficient ζ [46]. Parameters c_1 and c_2 of the discrete dashpot elements at both ends of the beam bridge accounting for geometrical damping are derived by utilizing the so-called Wolf cone model based on the subsoil properties [46]. The Wolf cone model is also used for the evaluation of the discrete spring coefficients k_1 and k_2, for the torsional spring coefficients k_3 and k_4 accounting for the influence of the bending stiffness of the rails, and for the lumped masses m_1 and m_2, respectively [46]. In order to avoid unlikely low damping values log-normally distributed damping coefficient ζ is truncated at $\zeta = 0.05\%$. Furthermore track irregularities, which are modelled as random field representing deviations in vertical direction from the perfect rail, are considered as source of uncertainty related with the excitation of the structure.

Track irregularities, assuming to represent a stationary Gaussian stochastic process, are modelled through random irregular track profile functions $I_r(x)$, which are superposed to the beam deflection and generated by the superposition of random $J = 1000$ harmonic functions as described in [50]. The uppermost frequency of the considered harmonic functions is $\Omega_u = 2.1$ rad/m, and the lowermost frequency is $\Omega_l = 0.07$ rad/m, respectively. Solving the bridge–train interaction problem allows for considering the influence of track irregularities. In Table 1, the uncertainties considered in the system response evaluation and in the prediction of failure probabilities p_f for the low-fidelity and the high-fidelity model are listed with their corresponding random distribution as well as the mean value (Mean) and coefficient of variation CV.

The limiting factor in the dynamic design of railway bridges for the serviceability limit state (SLS) commonly is the bridge deck acceleration with possible consequence of ballast instability [9,43]. The design guideline Eurocode [9] recommends an acceleration limit value of 3.5 m/s^2 associated with ballast instability and 5.0 m/s^2 for ballastless track, respectively. Additionally for SLS, a failure probability of $p_{f_\mathrm{SLS}} = 10^{-3}$ must not be exceeded [43]. Quite naturally in this contribution the bridge deck acceleration $\ddot{w}(x,t)$ [cf. Eq. (24)] is considered as governing response quantity and the failure probability of the bridge structure is evaluated in dependency of bridge deck acceleration limit $\gamma = a_\mathrm{limit}$. In the

Table 1 Random variables

Variable	Distribution	Unit	Mean (CV)	Min–Max
Damping ζ	Trunc. log-norm.	%	0.5 (0.3)	–
Moment of inertia I	Gaussian	m^4	0.156 (0.1)	–
Young's modulus of subsoil E_s	Gaussian	GPa	400 (0.2)	
Poisson's ratio of subsoil ν_s	Gaussian	–	0.25 (0.1)	
Density of subsoil ρ_s	Gaussian	kg/m^3	2367 (0.1)	
Bedding modulus k	Gaussian	GPa	175 (0.1)	
Irregularly profile I_r	Stochastic process			
Phase angle φ_m	Uniform	rad	–	$0–2\pi$
Amplitude Q	Uniform	radm	–	0.592×10^{-6}–1.586×10^{-6}

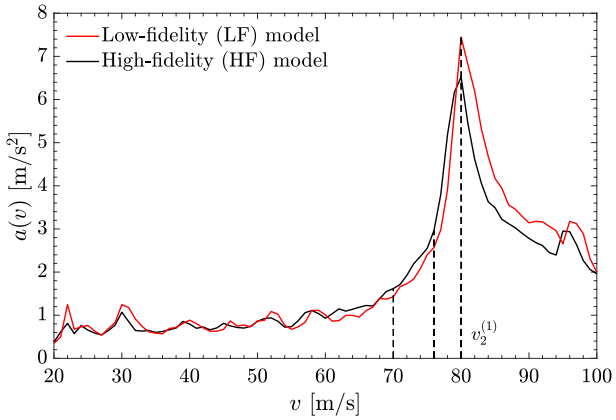

Fig. 4 Mean value acceleration spectrum of the low-fidelity (LF) model (red line) and the high-fidelity (HF) model (black line) accounting for uncertain damping ζ for a train speed range from $v = 20$ m/s to $v = 100$ m/s, respectively (Color figure online)

FORM and model-correction-based evaluation approach, the absolute maximum bridge deck acceleration $a(v) = \max\{\|\ddot{w}(x,t,v)\| : 0 \le x \le L,\ 0 \le t \le T\}$ at train speed v, location $0 \le x \le L$, and time $0 \le t \le T$ is used as governing response quantity. Structural failure is present if the limit state function of the uncertain time-dependent bridge beam structure is $g(a_{\text{limit}}, v) = a_{\text{limit}} - a(v) \le 0$. The model-correction-based reliability analysis algorithm is terminated when the evaluated reliability index $\hat{\beta}_{\text{HF}}^{(k)}$ of the current iteration does not diverge more than tolerance $\text{tol} = 10^{-3}$ from the reliability index $\hat{\beta}_{\text{HF}}^{(k-1)}$ of the previous step, i.e. $\|\hat{\beta}_{\text{HF}}^{(k-1)} - \hat{\beta}_{\text{HF}}^{(k)}\| \le \text{tol}$.

3.3 Failure probability evaluation

Damping with a Pearson correlation coefficient r [51] of $r_{\zeta_{\text{LF}}} = 0.69$ for the LF model considering moving single forces and $r_{\zeta_{\text{HF}}} = 0.65$ for the HF model accounting for the moving train as MSD system at train speed $v = 70$ m/s is the most influential random variable on the structural responses. Consequently, in a preliminary evaluation of the failure probabilities the model-correction-based approach is applied considering ζ as only source of uncertainty. The correlation coefficients are computed by crude Monte Carlo simulations with a sample size of $N_{\text{MC}} = 500$ for the LF and the HF model, respectively. Failure probability $\hat{p}_{f_{\text{HF}}}$ of the corrected LF model is determined with the corresponding reliability index $\hat{\beta}_{\text{HF}}$ and the standard normal cumulative distribution function $\Phi(x)$, $\hat{p}_{f_{\text{HF}}} = \Phi(-\hat{\beta}_{\text{HF}})$. Failure probabilities in the range of 10^{-6} to 10^{0} are of interest in this study as according to Eurocode [52] p_f must be limited to $p_f = 10^{-3}$ for serviceability limit state (SLS), and for ultimate limit state (ULS) $p_f = 10^{-6}$ must not be exceeded.

Considering the mean value of the uncertain damping parameter ζ the maximum of $a(v)$ appears at train speed $v = 80$ m/s, close to the second resonance speed of the first mode $v_2^{(1)} = 75.1$ m/s, with $a_{\max_{\text{LF}}}(80) = 7.45\,\text{m/s}^2$ for the LF model and $a_{\max_{\text{HF}}}(80) = 6.52\,\text{m/s}^2$ for the HF model (cf. Fig. 4).

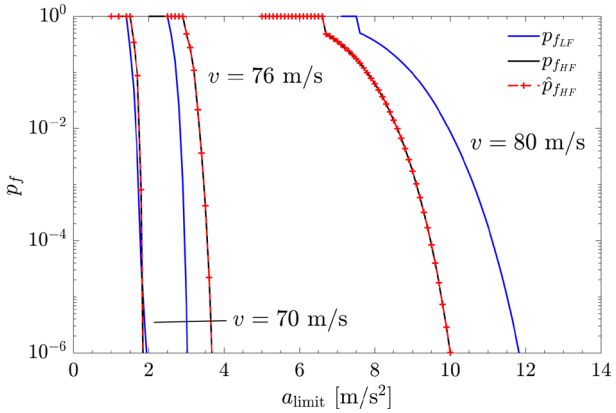

Fig. 5 Failure probability $p_{f_{\text{LF}}}$ evaluated based on the first-order reliability method (FORM) for the low-fidelity (LF) model and $p_{f_{\text{HF}}}$ for the high-fidelity (HF) model, and $\hat{p}_{f_{\text{HF}}}$ based on the model-correction method for train speeds $v = 70$ m/s, $v = 76$ m/s, and $v = 80$ m/s depicted over the acceleration limit a_{limit}

Consequently, p_{f} is evaluated at train speed $v = 80\,\text{m/s}$, which is close to resonance speed $v_2^{(1)}$, at $v = 80\,\text{m/s}$ the maximum bridge deck acceleration occurs, and maximum p_{f} is expected for the LF model and the HF model, respectively. Additional train speeds at which p_{f} is evaluated are $v = 70\,\text{m/s}$ ($v = 70\,\text{m/s}$ leads to the maximum acceleration considering six uncertain parameters) and $v = 76\,\text{m/s}$.

As starting point for the FORM algorithm $u_0 = 0.01$ is chosen, which is the initial value for ζ in standard normal space. The determination of the failure probability $p_{f_{\text{LF}}}$ of the LF modelling approach considering a train speed of $v = 70$ m/s takes $t = 36$ s and is resulting in $p_{f_{\text{LF}}} = 0.048$ when applying FORM. For the sophisticated HF bridge–train interaction model the evaluation of the failure probability $p_{f_{\text{HF}}} = 0.342$ takes $t = 1880$ s based on FORM. When applying the model-correction-based approach considering train speed $v = 70$ m/s failure probability of $\hat{p}_{f_{\text{HF}}} = 0.342$ is evaluated with computation time $t = 1030$ s. While achieving an approximately equal failure probability $\hat{p}_{f_{\text{HF}}} \approx p_{f_{\text{HF}}}$, the computation time can be reduced by 45.2% when utilizing the model-correction-based approach. In Fig. 5, the failure probability $p_{f_{\text{LF}}}$ for the LF modelling approach evaluated with FORM, $p_{f_{\text{HF}}}$ for the HF modelling approach evaluated with FORM, and $\hat{p}_{f_{\text{HF}}}$ for the HF modelling approach evaluated based on the model-correction method are depicted over the acceleration threshold a_{limit}. For trains speeds $v = 76$ m/s and $v = 80$ m/s, the failure probabilities $p_{f_{\text{HF}}}$ of the HF analysis model evaluated with FORM match the failure probabilities $\hat{p}_{f_{\text{HF}}}$ of the corrected LF model when the model-correction-based approach is applied.

Considering six uncertain parameters the mean value acceleration response spectrum of the LF model (red line) and the HF model (black line) is depicted in Fig. 6 for a train speed range from $v = 20$ m/s to $v = 100$ m/s. Additionally Fig. 6 shows the mean value spectrum of the HF model including track irregularities (blue line). Maximum bridge deck acceleration $a(v)$ of the LF model, the HF model, and the HF model including track irregularities of $a_{\max_{\text{LF}}}(70) = 4.32\,\text{m/s}^2$, $a_{\max_{\text{HF}}}(70) = 3.36\,\text{m/s}^2$, and $a_{\max_{\text{HFtrackirr}}}(70) = 3.56\,\text{m/s}^2$ occur at train speed $v = 70$ m/s, which is close to the third resonance speed of the second mode $v_2^{(3)} = 72.4$ m/s.

The failure probabilities of the LF model, the HF model, and the HF model considering track irregularities are evaluated at train speed $v = 70$ m/s, where the maximum bridge deck acceleration occurs and the largest failure probability is expected. Additionally p_{f} is evaluated at $v = 76$ m/s and $v = 80$ m/s. Figure 7a depicts failure probabilities p_{f} of the LF model ($p_{f_{\text{LF}}}$, blue line) and the HF model ($p_{f_{\text{HF}}}$, black circles) based on FORM, and of the HF model ($\hat{p}_{f_{\text{HF}}}$, red line with $+$ markers) predicted with the model-correction-based approach.

The FORM algorithm is initially started at $\mathbf{u}_0 = (0.01, 0.01, 0.01, 0.01, 0.01, 0.01)$. Failure probabilities $p_{f_{\text{HF}}}$ of the high-fidelity model evaluated for distinct acceleration limits a_{limit} are in agreement with $\hat{p}_{f_{\text{HF}}}$-predictions utilizing the model-correction-based approach. At train speed $v = 80$ m/s, predicted failure probabilities $\hat{p}_{f_{\text{HF}}} = 0.202$ and $\hat{p}_{f_{\text{HF}}} = 0.057$ utilizing FORM for $a_{\text{limit}} = 2.5\,\text{m/s}^2$ and $a_{\text{limit}} = 3\,\text{m/s}^2$ correspond with the $p_{f_{\text{HF}}}$ results obtained by FORM. Failure probabilities $\hat{p}_{f_{\text{HF}}}$ evaluated with the model-correction algorithm are compared with $p_{f_{\text{HF}}}$-predictions for acceleration limits $a_{\text{limit}} = 4\,\text{m/s}^2$, and $5\,\text{m/s}^2$ at train speed $v = 70$ m/s, and $a_{\text{limit}} = 6,\ 7,\ 8.5,$ and $9\,\text{m/s}^2$ for train speed $v = 76$ m/s. The comparison shows that predictions of both $\hat{p}_{f_{\text{HF}}}$ and $p_{f_{\text{HF}}}$ are in agreement, respectively.

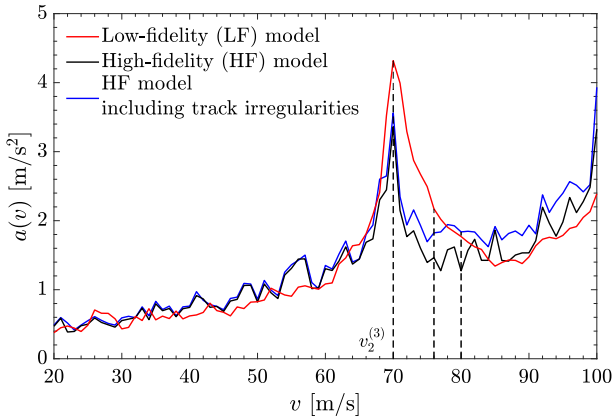

Fig. 6 Mean value acceleration spectrum of the low-fidelity (LF) model (red line) and the high-fidelity (HF) model (black line) considering six random variables, respectively, and the HF model accounting for track irregularities (blue line) for a train speed range from $v = 20$ m/s to $v = 100$ m/s (Color figure online)

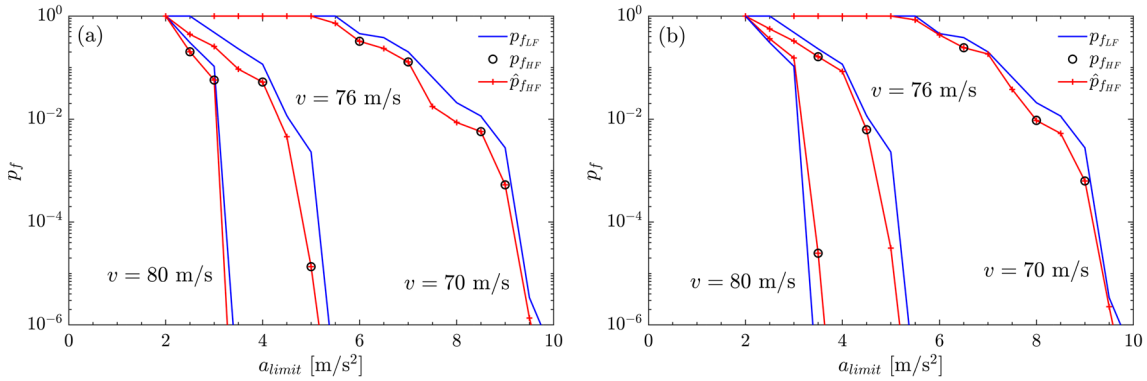

Fig. 7 Failure probabilities evaluated based on the first-order reliability method (FORM) for the low-fidelity (LF) model $p_{f_{\mathrm{LF}}}$ and the high-fidelity (HF) model $p_{f_{\mathrm{HF}}}$, and $\hat{p}_{f_{\mathrm{HF}}}$ based on the model-correction method for train speeds $v = 70,\ 76,$ and 80 m/s depicted over the acceleration limit a_{limit} **a** considering six random variables and **b** additionally accounting for track irregularities

The LF model results in higher p_{f}-predictions for the same a_{limit} compared with the HF model indicating higher acceleration responses and consequently a more conservative modelling approach. At a train speed of $v = 76$ m/s and $a_{\mathrm{limit}} = 7$ m/s^2, the LF model provides $p_{f_{\mathrm{LF}}} = 0.201$ and $\hat{p}_{f_{\mathrm{HF}}} = 0.128$ resulting an a difference of 36.3 %. It should be noted that when six random variables are considered, the beam bridge is viscoelastically supported and soil–structure interaction (SSI) is considered resulting in structural responses and failure probabilities that are significantly different than shown in Fig. 5 where a simply supported beam bridge is considered.

In the presence of track irregularities, failure probabilities of the HF model are slightly increased, for example, for $v = 70$ m/s $p_{f_{\mathrm{HF}}} = \hat{p}_{f_{\mathrm{HF}}} = 5.287 \times 10^{-4}$ neglecting track irregularities and $p_{f_{\mathrm{HF}}} = \hat{p}_{f_{\mathrm{HF}}} = 6.287 \times 10^{-4}$ accounting for track irregularities (cf. Fig. 7b). In particular at a train speed of $v = 80$ m/s, the failure probability of the HF fidelity model exceeds the failure probability of the LF model. For $a_{\mathrm{limit}} = 3$ m/s^2, failure probability of the LF model is with $p_{f_{\mathrm{LF}}} = 0.105$ 31.4% lower than $\hat{p}_{f_{\mathrm{HF}}} = 0.153$. Failure probabilities of the HF model ($p_{f_{\mathrm{HF}}}$, black circles) are evaluated for the considered train speeds $v = 70$ m/s ($a_{\mathrm{limit}} = 3.5$ m/s^2), $v = 76$ m/s ($a_{\mathrm{limit}} = 3.5,\ 4.5$ m/s^2), $v = 80$ m/s ($a_{\mathrm{limit}} = 6.5,\ 8,\ 9$ m/s^2) match the model-correction-based p_{f}-predictions ($\hat{p}_{f_{\mathrm{HF}}}$, red line with + markers).

3.4 Convergence rate of the model-correction-based algorithm and correlation between the multifidelity models

When considering damping ζ as only source of uncertainty the LF analysis model and the HF analysis model are with a Pearson correlations coefficient of $r_{\mathrm{LF-HF}} = 0.9998$ for $v = 70$ m/s, $r_{\mathrm{LF-HF}} = -0.9995$ for $v = 76$ m/s, and $r_{\mathrm{LF-HF}} = 0.9999$ for $v = 80$ m/s highly correlated and as a consequence the model-correction-based algorithm typically converges after 5–7 iterations based on the convergence criterion provided in Sect. 3.2. In correspondence with the convergence behaviour $N_{\mathrm{HF}} = 5$–7 computationally demanding evaluations of limit state function g_{HF} are required, whereas when applying the FORM method with the HF model, for example, for a train speed $v = 80$ m/s and $a_{\mathrm{limit}} = 9$ m/s^2 $N_{\mathrm{HF}} = 30$ evaluations of g_{HF} are required with a computational time of $t = 85$ min and 43 s. At $v = 80$ m/s and $a_{\mathrm{limit}} = 9$ m/s^2, the model-correction-based approach requires $N_{\mathrm{HF}} = 6$ evaluations of g_{HF} resulting in an analysis time of $t = 18$ min and 25 s, which is a reduction of 78.4%.

Pearson correlation coefficients accounting for six random variables (cf. Table 1) in the structural response evaluation are $r_{\mathrm{LF-HF}} = 0.9281$, $r_{\mathrm{LF-HF}} = -0.9624$, and $r_{\mathrm{LF-HF}} = 0.9473$ for train speeds $v = 70$ m/s, $v = 76$ m/s, and $v = 80$ m/s, respectively. Convergence of the model-correction-based approach when the six random variables are considered occurs after 6–9 iterations utilizing the introduced convergence criterion. With convergence after 6 iterations and $N_{\mathrm{HF}} = 6$ evaluations of g_{HF} at $v = 80$ m/s and $a_{\mathrm{limit}} = 3$ m/s^2 the model-correction-based approach takes $t = 17$ min and 24 s and is 81.3% faster than FORM for computing $p_{f_{\mathrm{HF}}}$ with $N_{\mathrm{HF}} = 33$ required evaluations of g_{HF} and $t = 93$ min and 23 s. When considering $v = 70$ m/s and $a_{\mathrm{limit}} = 9$ m/s^2, the model-correction-based approach requires 9 iterations for convergence and an analysis time $t = 26$ min and 12 s, which is 72.9% more efficient than prediction $p_{f_{\mathrm{HF}}}$ utilizing FORM with $N_{\mathrm{HF}} = 34$ limit state function evaluations with an analysis time $t = 96$ min and 46 s. Accounting for six random variables and track irregularities results in a slight reduction of the correlation between the LF and the HF model, however with Pearson correlation coefficients of $r_{\mathrm{LF-HF}} = 0.9032$, $r_{\mathrm{LF-HF}} = -0.9118$, and $r_{\mathrm{LF-HF}} = 0.9341$ for $v = 70$ m/s, $v = 76$ m/s, and $v = 80$ m/s the models are still highly correlated. Hence the LF model captures the fundamental physical behaviour of the HF model well. Convergence of the model-correction-based method for $v = 76$ m/s and $a_{\mathrm{limit}} = 3.5$ m/s^2 is reached after 7 iterations and an analysis time $t = 20$ min and 22 s for $N_{\mathrm{HF}} = 7$ limit state function evaluations of g_{HF}. FORM requires $N_{\mathrm{HF}} = 34$ limit state function evaluations of g_{HF} and $t = 97$ min and 2 s for $v = 76$ m/s and $a_{\mathrm{limit}} = 3.5$ m/s^2 resulting in an increase of 376.4% in the analysis time. At $v = 70$ m/s for $a_{\mathrm{limit}} = 8.5$ m/s^2 10, iterations are required for convergence of the model-correction based approach and an analysis time of $t = 28$ min and 23 s for $N_{\mathrm{HF}} = 10$ computationally demanding limit state function evaluations of g_{HF}. The FORM algorithm requires $N_{\mathrm{HF}} = 36$ evaluations of g_{HF} and an analysis time of $t = 103$ min and 10 s, which is an increase of 263.6% in the analysis time.

The model-correction-based algorithm shows a slightly impaired convergence rate when considering six random variables and track irregularities. When analysing the convergence rate of the model-correction-based algorithm based on the introduced convergence criterion and the correlation coefficient of the LF and the HF model (cf. Fig. 8), it can be seen that the convergence of the algorithm is slightly reduced for a reduction in the correlation coefficient.

In Table 2, the convergence behaviour of the model-correction-based algorithm at $v = 76$ m/s is provided when considering structural damping ζ as stochastic variable. With a failure probability of $\hat{p}_{f_{\mathrm{HF}}} = 4.188 \times 10^{-4}$ after seven iterations of the model-correction-based algorithm $\hat{p}_{f_{\mathrm{HF}}}$ is of 0.9% smaller than $p_{f_{\mathrm{HF}}} = 4.226 \times 10^{-4}$ evaluated with the FORM procedure at $v = 76$ m/s with $a_{\mathrm{limit}} = 3.5$ m/s^2. Consequently, seven evaluations of the HF model limit state function are required for prediction of $\hat{p}_{f_{\mathrm{HF}}}$ at $v = 76$ m/s with $a_{\mathrm{limit}} = 3.5$ m/s^2 when using the model-correction-based approach with total analysis time of $t = 21$ m 12 s, whereas when applying FORM $p_{f_{\mathrm{HF}}}$ $n_{\mathrm{HF}} = 31$ limit state function evaluations of the computationally demanding HF model are required leading to an 77.3% increased analysis time of $t = 93$ m 15 s.

4 Conclusion

In this contribution, a model-correction-based analysis approach based on the first-order reliability method (FORM) has been introduced for efficient reliability assessment of uncertain dynamical systems and applied to an application example. The model-correction-based algorithm aims to calibrate a low-fidelity (LF) model to an elaborate high-fidelity (HF) model close to the most probable point (MPP) in standard normal space such

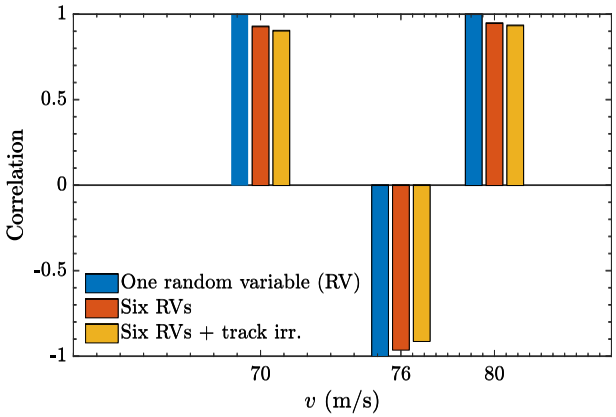

Fig. 8 Pearson correlation coefficient of low-fidelity and high-fidelity analysis model including six random variables and additionally accounting for track irregularities

Table 2 Zero-order model-correction-based approach at train speed $v = 76$ m/s and $a_{\text{limit}} = 3.5$ m/s^2 considering uncertain structural damping ζ

Variable	1st iteration	2nd iteration	3rd iteration	4th iteration	5th iteration	6th iteration	7th iteration
Damping ζ	-3.912	-3.127	-3.427	-3.301	-3.353	-3.331	-3.340
Capacity factor κ_{HF}	0.958	1.023	0.991	1.994	0.999	1.001	0.999
Reliability index β	3.912	3.127	3.428	3.301	3.353	3.331	3.340
Failure probability $\hat{p}_{f_{\text{HF}}}$	4.575×10^{-5}	8.836×10^{-4}	3.043×10^{-4}	4.813×10^{-4}	4.004×10^{-4}	4.320×10^{-4}	4.188×10^{-4}

that the calibrated LF model provides an accurate estimate of the failure probability for the computationally demanding HF model.

In an application example, reliability analysis of an existing railway bridge subjected to a high-speed train was performed based on two models with different degree of sophistication, a simplified low-fidelity (LF) model and a sophisticated high-fidelity (HF) model explicitly accounting for bridge–train interaction, respectively. The Euler–Bernoulli beam bridge model with extended boundary conditions accounts for soil–structure interaction (SSI) and the structural responses has been determined by complex modal analysis due to non-classical damping of the beam bridge. While the low-fidelity model accounting for the passing train as moving single forces representing the static axle loads of the train enables an computational efficient structural response evaluation in the high-fidelity modelling approach the passing train is modelled as mass-spring-damper (MSD) system considering bridge–train interaction and the effects of track irregularities, however limit state function evaluations are computationally demanding. In a preliminary study structural damping has been considered as only source of uncertainty, resulting in highly correlated models and consequently in fast convergence rates of the model-correction-based algorithm for the computation of failure probabilities for three different train speeds over varying bridge deck acceleration limits. When considering six random variables and additionally track irregularities correlation of the models was slightly reduced, however the evaluated correlation between the models was still high. It was demonstrated that the convergence rate of the model-correction-based algorithm is influenced by the correlation of the LF and HF model. In case of a minor reduction of the correlation, the applied approach showed slightly reduced convergence rates. Due to the substantial correlation of the analysis models, the governing physical properties leading to structural failure were appropriately captured by the LF model, hence fast convergence of the iterative technique was achieved, an accurate failure probability has been obtained after few iterations, and the HF model had to be evaluated only a few times for calibrating the LF model. It has been demonstrated that the model-correction-based approach significantly decreased the analysis time for reliability assessment of the sophisticated HF model accounting for bridge–train interaction, while leading to accurate failure probability predictions.

An investigation of the model-correction-based approach considering less correlated low-fidelity models, considering multiple low-fidelity models and optimal distribution of limit state function evaluations, and a comparison with multifidelity Monte Carlo techniques in terms of accuracy and efficiency is of interest for future research.

Acknowledgements Funding of the International Research Training Group (IRTG) 2657 by DFG is gratefully acknowledged (Grant Reference Number 433082294)

Funding Open Access funding enabled and organized by Projekt DEAL.

Appendix A First-order reliability method

Before applying the FORM algorithm, the problem setup, i.e. the limit state function and the problem related random variable need to be defined. Therefore, typically the Rosenblatt transformation in combination with the Nataf-Model is used $U_i = \Phi^{-1}(F_i(X_i \mid X_1))$ [4]. Most probable point (MPP) $\mathbf{u}^*$ is defined as the point in the failure set F with the largest probability density, that is, the closest point on the failure surface $g(\mathbf{u}) = 0$ to the origin $\mathbf{O}$ in standard normal space [53]. In order to determine $\mathbf{u}^*$ in standard normal space which coincide with the design point x^* in original space an optimization problem [4]

$$\mathbf{u}^* = \operatorname{argmin}\left(\frac{1}{2}\mathbf{u}^{\mathrm{T}}\mathbf{u}\right); \qquad \text{subjet to}: \; g[\mathbf{x}(\mathbf{u})] = 0 \tag{A1}$$

has to be solved. Therefore, different optimization algorithms, for example, the SQP algorithm implemented as fmincon-function in MATLAB and the so-called Hasofer–Lind–Rackwitz–Fiessler (HLRF) algorithm can be applied. The HLRF algorithm is an iterative gradient-based optimization approach adapted to this type of reliability problems [54]. By applying an optimization procedure, the most probable point $\mathbf{u}^*$ is determined [4]

$$\mathbf{u}^* = \beta\boldsymbol{\alpha}^* \tag{A2}$$

with the reliability index β, which is the distance between MPP $\mathbf{u}^*$ and O, and unit normal vector $\boldsymbol{\alpha}^* = \frac{\nabla g}{|\nabla g|}$. Approximating the actual limit state surface $g(\mathbf{u}) = 0$ by its tangent hyperplane [4]

$$g(\mathbf{u}) = \beta + \boldsymbol{\alpha}^{\mathrm{T}}\mathbf{u} \tag{A3}$$

yields the approximation of failure probability p_{f},

$$p_{\mathrm{f}} \approx \Phi(-\beta) \tag{A4}$$

Equation (A4) provides the first-order approximation of the failure probability p_{f} and β is the corresponding first-order approximation to the reliability index. The accuracy of the method depends on how well the true failure surface is represented by the linear approximation. If $g(\mathbf{u})$ is linear, the FORM procedure leads to the exact result [4].

Consideration of time-dependent limit state functions the constrained optimization problem of the FORM method reads [41]

$$\mathbf{u}^*(\gamma, t) = \operatorname{argmin}\{\|\mathbf{u}\| \;\mid\; g(\mathbf{u}, \gamma, t) = 0\} \tag{A5}$$

Consequently for dynamical systems, a first-order approximation of the tail probability is given as [41]

$$P(\gamma \leq Z(t, \mathbf{u})] \approx \Phi[-\beta(\gamma, t)] \tag{A6}$$

with reliability index $\beta(\gamma, t) = \boldsymbol{\alpha}(\gamma, t)\mathbf{u}^*(\gamma, t)$, where $\boldsymbol{\alpha}(\gamma, t) = -\nabla_{\mathbf{u}} g(\mathbf{u}^*, x, t)/\|\nabla_{\mathbf{u}} g(\mathbf{u}^*, \gamma, t)\|$ represents the negative normalized gradient vector of limit state function $g(\mathbf{u}, \gamma, t)$ at most probable point $\mathbf{u}^*$ (cf. Fig. 9).

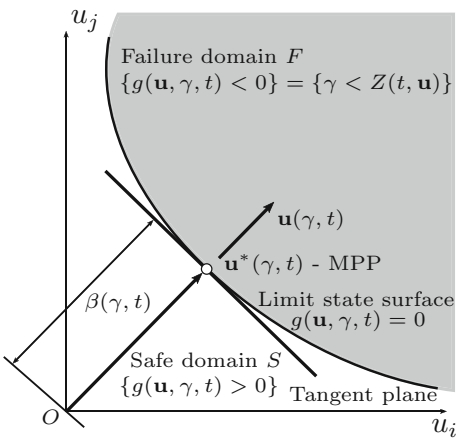

Fig. 9 First-order reliability method (FORM) accounting for time-dependent systems, modified from [41]

References

1. Moustapha, M., Marelli, S., Sudret, B.: Active learning for structural reliability: survey, general framework and benchmark. Struct. Saf. **96**, 102174 (2022)
2. Hasofer, A.M., Lind, N.C.: Exact and invariant second-moment code format. J. Eng. Mech. Div. **100**(1), 111–121 (1974)
3. Melchers, R.E.: Structural Reliability Analysis and Prediction, 2nd edn. Wiley, Hoboken (1999)
4. Bucher, C.: Computational Analysis of Randomness in Structural Mechanics. CRC Press, Boca Raton (2009)
5. Ditlevsen, O., Madsen, H.O.: Structural Reliability Methods. Wiley, Hoboken (1996)
6. Madsen, H.O., Krenk, S., Lind, N.C.: Methods of Structural Safety, 2nd edn. Dover Publications, Mineola (2006)
7. Melchers, R., Beck, A.: Structural Reliablity Analysis and Prediction, 3rd edn. Wiley, Hoboken (2018)
8. Allahvirdizadeh, R., Andersson, A. Karoumi R.: Proceedings of the XI International Conference on Structural Dynamics (EURODYN 2020), Athens, Greece (2020)
9. Eurocode 1. EN 1991-2: Eurocode 1: Actions on Structures (2003)
10. Madsen, H.O.: Omission sensitivity factors. Struct. Saf. **5**, 35–45 (1988)
11. Breitung, K.: Asymptotic approximations for multinormal integrals. J. Eng. Mech. **110**, 357–366 (1984)
12. Der Kiureghian, A., Lin, H., Hwang, S.: Second-order reliability approximations. J. Eng. Mech. **113**(8), 1208–1225 (1987)
13. Lemaire, M.: Structural Reliability. ISTE Ltd., London (2009)
14. Tvedt, L.: Distribution of quadratic forms in normal space—application to structural reliability. J. Eng. Mech. **116**(6), 1183–1197 (1990)
15. Der Kiureghian, A., Dakessian, T.: Multiple design points in first and second-order reliability. Struct. Saf. **20**, 37–49 (1998)
16. Hu, Z., Du, X.: First order reliability method for time-variant problems using series expansion. Struct. Multidiscip. Optim. **51**, 1–21 (2015)
17. Hagen, Ø., Tvedt, L.: Vector process out-crossing as parallel system sensitivity measure. J. Eng. Mech. **117**(10), 2201–2220 (1991)
18. Hu, Z., Du, X.: Reliability analysis for hydrokinetic turbine blades. Renew. Energy **48**, 251–262 (2012)
19. Bucher, C., Most, T.: A comparison of approximate response functions in structural reliability analysis. Probab. Eng. Mech. **23**, 154–163 (2008)
20. Bucher, C., Bourgund, U.: A fast and efficient response surface approach for structural reliability problems. Struct. Saf. **7**, 57–66 (1990)
21. Myers, R.H.: Response surface methodology—current status and future directions. J. Qual. Technol. **31**(1), 30–44 (1999)
22. Iourtchenko, D., Mo, E., Naess, A.: Reliability of strongly nonlinear single degree of freedom dynamic systems by the path integration method. J. Appl. Mech. **75**, 061016-1–061016-8 (2008)
23. Naess, A., Iourtchenko, D., Batsevych, O.: Reliability of systems with randomly varying parameters by the path integration method. Probab. Eng. Mech. **26**(1), 5–9 (2011)
24. Petromichelakis, I., Kougioumtzoglou, I.A.: Addressing the curse of dimensionality in stochastic dynamics: a wiener path integral variational formulation with free boundaries. Proc. R. Soc. A Math. Phys. Eng. Sci. **476**(2243), 20200385 (2020)
25. Zhang, J.: Modern Monte Carlo methods for efficient uncertainty quantification and propagation: a survey. WIREs Comput. Stat. **13**(5), e1539 (2021)
26. Peherstorfer, B., Willcox, K., Gunzburger, M.: Survey of multifidelity methods in uncertainty propagation, inference, and optimization. SIAM Rev. **60**(3), 550–591 (2018)
27. Peherstorfer, B., Willcox, K., Gunzburger, M.: Optimal model management for multifidelity Monte Carlo estimation. SIAM J. Sci. Comput. **38**(5), A3163–A3194 (2016)
28. Tao, J., Sun, G.: Application of deep learning based multi-fidelity surrogate model to robust aerodynamic design optimization. Aerosp. Sci. Technol. **92**, 722–737 (2019)
29. Perdikaris, P., Venturi, D., Royset, J.O., Karniadakis, G.E.: Multi-fidelity modelling via recursive co-kriging and Gaussian–Markov random fields. Proc. R. Soc. A Math. Phys. Eng. Sci. **471**(2179), 20150018 (2015)

30. Fernández Godino, M.G., Park, C., Kim, N.H., Haftka, R.T.: Issues in deciding whether to use multifidelity surrogates. AIAA J. **57**(5), 2039–2054 (2019)
31. Proppe, C.: Multifidelity reliability estimation. PAMM Proc. Appl. Math. Mech. **19**(1), e201900466 (2019)
32. Guyader, A., Hengartner, N., Matzer-Lober, E.: Simulation and estimation of extreme quantiles and extreme probabilities. Appl. Math. Optim. **64**(2), 171–196 (2011)
33. Walter, C.: Moving particles: a parallel optimal multilevel splitting method with application in quantiles estimation and meta-model based algorithms. Struct. Saf. **55**, 10–25 (2015)
34. Proppe, C.: A multilevel moving particles method for reliability estimation. Probab. Eng. Mech. **59**, 103018 (2020)
35. Proppe, C.: The moving particles method for reliability estimation: recent advances. PAMM Proc. Appl. Math. Mech. **20**(1), e202000295 (2021)
36. Proppe, C., Kaupp, J.: On information fusion for reliability estimation with multifidelity models. Probab. Eng. Mech. **69**, 103291 (2022)
37. Dhulipala, S., Shields, M., Spencer, B., Bolisetti, C., Slaughter, A., Labouré, V., Chakroborty, P.: Active learning with multifidelity modeling for efficient rare event simulation. J. Comput. Phys. **468**, 111506 (2022)
38. Ditlevsen, O., Arnbjerg-Nielsen, T.: Model-correction-factor method in structural reliability. J. Eng. Mech. **120**(1), 1–10 (1994)
39. Dimitrov, D., Friis-Hansen, P., Berggreen, C.: 17th International Conference on Composite Materials (ICCM-17), Edinburgh, United Kingdom (2009)
40. Franchin, P., Ditlevsen, O., Der Kiureghian, A.: Model correction factor method for reliability problems involving integrals of non-Gaussian random fields. Probab. Eng. Mech. **17**, 109–122 (2002)
41. Alibrandi, U., Der Kiureghian, A.: A gradient-free method for determining the design point in nonlinear stochastic dynamic analysis. Probab. Eng. Mech. **28**, 2–10 (2012)
42. Hirzinger, B.: Contributions to modeling and reliability assessment strategies in railway bridge dynamics. Ph.D. thesis, University of Innsbruck (2020)
43. Hirzinger, B., Adam, C., Salcher, P., Oberguggenberger, M.: On the optimal strategy of stochastic based reliability assessment of railway bridges for high-speed trains. Meccanica **54**(9), 1385–1402 (2019)
44. Yang, Y.B., Yau, J.D., Wu, Y.S.: Vehicle-Bridge Interaction Dynamics. World Scientific Publishing Co. Pte. Ltd., Singapore (2004)
45. Clough, R.W., Penzien, J.: Dynamics of Structures, 2nd edn. McGraw-Hill Inc., New York (1993)
46. Hirzinger, B., Adam, C., Salcher, P.: Dynamic response of a non-classically damped beam with general boundary conditions subjected to a moving mass-spring-damper system. Int. J. Mech. Sci. **185**, 105877 (2020)
47. Salcher, P., Adam, C.: Modeling of dynamic train–bridge interaction in high-speed railways. Acta Mech. **226**(8), 2473–2495 (2015)
48. König, P., Salcher, P., Adam, C., Hirzinger, B.: Dynamic analysis of railway bridges exposed to high-speed trains considering the vehicle–track–bridge–soil interaction. Acta Mech. **232**, 4583–4608 (2021)
49. Ju, S.H., Lin, H.T.: Resonance characteristics of high-speed trains passing simply supported bridges. J. Sound Vib. **267**(5), 1127–1141 (2003)
50. König, P., Salcher, P., Adam, C.: An efficient model for the dynamic vehicle–track–bridge–soil interaction system. Eng. Struct. **253**, 113769 (2022)
51. Helton, J.C., Johnson, J.D., Sallaberry, C.J., Storlie, C.B.: Survey of sampling-based methods for uncertainty and sensitivity analysis. Reliab. Eng. Syst. Saf. **91**(10–11), 1175–1209 (2006)
52. Eurocode 0. EN 1990: Eurocode 0: Basis of structural design (2003)
53. Bai, Y., Jin, W.: Marine Structural Design, 2nd edn. Elsevier, Amsterdam (2016)
54. Rackwitz, R., Fiessler, B.: Structural reliability under combined random load sequences. Comput. Struct. **9**, 489–494 (1978)